Influences of extratropical water masses on equatorial Pacific cold tongue variability during the past 160 ka as revealed by faunal evidence of planktic foraminifers

JQS

PAI-SEN YU,[1] MARKUS KIENAST,[2] MIN-TE CHEN,[1]* ISABEL CACHO,[3] JOS ABEL FLORES,[4] MAHYAR MOHTADI[5] and ALAN C. MIX[6]

[1]Institute of Applied Geosciences, National Taiwan Ocean University, Keelung 20224, Taiwan
[2]Department of Oceanography, Dalhousie University, Halifax, Nova Scotia, Canada
[3]Department of Stratigraphy, Paleontology, and Marine Geosciences, University of Barcelona, 08028 Barcelona, Spain
[4]Department of Geology, University of Salamanca, 37008 Salamanca, Spain
[5]Center for Marine Environmental Sciences (MARUM), University of Bremen, 28359 Bremen, Germany
[6]College of Oceanic and Atmospheric Sciences, Oregon State University, Corvallis, OR 97331, USA

ABSTRACT: Glacial cooling ($\sim$1–5°C) in the eastern equatorial Pacific (EEP) cold tongue is often attributed to increased equatorial upwelling, stronger advection from the Peru–Chile Current (PCC), and to the more remote subpolar southeastern Pacific water mass. However, evidence is scarce for identifying unambiguously which process plays a more important role in driving the large glacial cooling in the EEP. To address this question, here we adopt a faunal calibration approach using planktic foraminifers with a new compilation of coretop data from the eastern Pacific, and present new downcore variation data of fauna assemblage and estimated sea surface temperatures (SSTs) for the past 160 ka (Marine Isotope Stage (MIS) 6) from ODP Site 1240 in the EEP. With significant improvement achieved by adding more coretop data from the eastern boundary current, our downcore calibration results indicate that most of the glacial cooling episodes over the past 160 ka in the EEP are attributable to increased influence from the subpolar water mass from high latitudes of the southern Pacific. By applying this new calibration of the fauna SST transfer function to a latitudinal transect of eastern Pacific (EP) cores, we find that the subpolar water mass has been a major dynamic contributor to EEP cold tongue cooling since MIS 6. Copyright © 2012 John Wiley & Sons, Ltd.

KEYWORDS: sea surface temperature; eastern equatorial Pacific; cold tongue; upwelling; planktic foraminifer.

Introduction

The eastern equatorial Pacific (EEP) cold tongue is an area of cool tropical ocean surface caused by active upwelling driven by basin-scale trade winds. Sea surface temperature (SST) in the EEP is thus a sensitive indicator of the perturbations of surface winds and ocean currents in the Pacific, which are active components of the tropical air–sea interaction responsible for driving global climate variability on timescales of interannual to possibly millennial (Cane and Clement, 1999; Rutherford and D'Hondt, 2000; Ravelo, 2006; Clement and Peterson, 2008). Precise quantification of past SSTs in the EEP therefore offers important constraints for understanding how the EEP plays a role in driving such a wide spectrum of global climate variability.

Previous investigations of past SSTs in the EEP have applied various techniques, including planktic foraminifer stable isotopes (Koutavas and Lynch-Stieglitz, 2003), microfossil-based transfer functions (Pisias and Mix, 1997; Mix et al., 1999) and inorganic/organic geochemical proxies (e.g. Mg/Ca ratio in foraminiferal shells and alkenone unsaturation index) (Lea et al., 2000; Prahl et al., 2006; Kienast et al., 2006; Leduc et al., 2007). However, one of the important advantages of microfossil methods over purely chemical estimates of SST is that the faunal changes provide insights into oceanographic/water mass changes associated with the estimates of SSTs. More specifically, the coretop calibration-based Imbrie–Kipp transfer function method (IKTF) (Imbrie and Kipp, 1971) yields downcore factor assemblages that are defined on the basis of a coretop data matrix. The factor assemblages are therefore implicitly related to modern surface water masses and

hydrographic conditions. Even though the precision of IKTF estimates is vexed by problems of no-analogues and differential carbonate preservation states of planktic foraminifers (Andreasen and Ravelo, 1997; Mix et al., 1999), strategies have been developed for minimizing the SST biases associated with these problems (Prell, 1985; Mix et al., 1999; Feldberg and Mix, 2002; MARGO Project Members, 2009).

The magnitude of tropical cooling and the extent to which the response of the cold tongue are a function of tropical *versus* extratropical climate feedback and/or other boundary conditions are open questions still (Chiang, 2009). SST variability in the EEP is commonly explained by one of the following key mechanisms: shifts in the position of the intertropical convergence zone (ITCZ) (e.g. Pisias and Mix, 1997), coupled tropical atmosphere–ocean dynamics (La Niña/El Niño-like; Cane and Clement, 1999; Koutavas and Lynch-Stieglitz, 2003) or even an ocean thermostat response from north Atlantic deep water (NADW) production (Benway et al., 2006). In addition, more recent studies suggest an active role of southern high-latitude climate processes/cold-water inflow modulating EEP variability during the late Quaternary (Liu et al., 2008; Pena et al., 2008; Dubois et al., 2009; Martínez-Garcia et al., 2010). In particular, glacial cooling ($\sim$1–5°C) in the EEP cold tongue has been further explained by increased equatorial upwelling, stronger advection from the Peru–Chile Current (PCC) system, or by the more remote subpolar southeastern Pacific water mass (Martínez-Garcia et al., 2010). One source of the cooling in the EEP is from southern high-latitude cool waters that are transported through an ocean tunnel of the PCC; another source may be equatorial upwelling (Feldberg and Mix, 2002, 2003). The increased intrusion from the cold PCC and well-developed EEP cold tongue during the Last Glacial Maximum (LGM) coincides with a northward migration ($\sim$1° S) of the equatorial front, as inferred from faunal evidence (Martínez et al., 2003,

*Correspondence: M.-T. Chen, as above.
E-mail: mtchen@mail.ntou.edu.tw

2006). However, all these past studies are based on coretop datasets that have scarce samples from the PCC, the most critical observation area on which a robust argument could be made. A lack of good control on PCC may even exacerbate the 'no-analogues' problem in applying IKTF.

In this study, we aim to improve on these shortcomings by adding new PCC coretop data (Mohtadi *et al.*, 2005) and, based on these data, to develop a new IKTF and apply it to cores from ODP Site 1240 retrieved from a location in the EEP cold tongue ($0.02°$ N, $86.46°$ W; water depth 2921 m; Mix *et al.*, 2003) (Fig. 1). Site ODP 1240 is located at the northwestern reaches of the cold tongue, in the equatorial front, and has an annual mean SST of 24.3°C (seasonal range of $\sim 2°$C) (Locarnini *et al.*, 2010). In this study, we present new data on planktic foraminifer assemblages and new fauna IKTF SST estimates spanning Marine Isotope Stage (MIS) 1–6 (approximately the past 160 ka). This new faunal record, combined with faunal records from nearby sites in the EEP cold tongue, is used to assess temporal and spatial changes in the oceanographic conditions in the EEP since MIS 6. The specific foci of this study are: (i) evaluating the sensitivity of the new faunal IKTF developed in this study for the EEP; (ii) identifying possible changes in water mass conditions (in particular PCC and subpolar components) that caused the variations in the faunal assemblages and the new IKTF SSTs at site ODP 1240; and (iii) interpreting SST variability and associated water mass exchanges in the EEP cold tongue since MIS 6 by applying the IKTF to published faunal records from more regions of the EEP.

Oceanographic background

The EEP cold tongue is a mix of cold-water masses upwelled mostly *in situ* from equatorial/divergence zones and advected from more remote extratropical waters in the southeastern Pacific. The water in the equatorial upwelling is sourced from the equatorial undercurrent (EUC), which originates in the southwestern Pacific (Subantarctic Mode Water) (Toggweiler *et al.*, 1991). The PCC inflow, which belongs to the eastern boundary current (EBC) system, is dynamically linked to the basin-scale Antarctic Circumpolar Current. The PCC upwelling occurs along the South American coast, which in turn carries cold and nutrient-rich water to the surface EEP via the South Equatorial Current near the eastern offshore area of the Galapagos. Ventilated cold subpolar water along the mid-latitude gyre provides another pathway for tropical–subtropical warm water mass exchange (Harper, 2000). On the Equator, the region of the cold tongue is restricted by warm-water masses of the western tropical Pacific and the eastern Pacific warm pool. Hence the juxtaposition of the nutrient-rich cold tongue (SST $< 24°$C; nitrate concentration $>10 \,\mu mol \, L^{-1}$) with the warm and nutrient-poor Equatorial Counter Current can be

observed in the EEP (Pak and Zaneveld, 1974; Pennington *et al.*, 2006).

The EEP cold tongue is characterized by low SST, a shallow thermocline and active upwelling that brings nutrient-rich subsurface water to the surface. These hydrographic conditions are intimately linked to the seasonal migration of the ITCZ (Fiedler and Talley, 2006; Pennington *et al.*, 2006). The expansion or shrinkage of the cold tongue is determined by the seasonal changes in the strength and asymmetric position of the trade winds (Fig. 1). The strongest northeasterly trade winds occur during the boreal winter as the ITCZ migrates to its southernmost location ($\sim 1°$ S) (Wyrtki, 1966, 1977; Amador *et al.*, 2006). During the boreal summer when the ITCZ is in its northernmost position ($\sim 9°$ N), the southeastern trade winds prevail and the cold tongue is at its greatest extent. The cold tongue variability exhibits its extremes on an interannual timescale (e.g. El Niño–Southern Oscillation).

Data and methods

Age model and faunal analysis

In the quest for an oxygen isotope-based chronology (e.g. SPECMAP type), a new age model with oxygen isotope stratigraphy (*Globigerinoides ruber*) (López-Otálvaro *et al.*, 2008) combined with 17 accelerator mass spectrometry (AMS) ^{14}C dating (Pena *et al.*, 2008) is established for ODP 1240 of this study. The AMS ^{14}C dating provided age controls on the interval of the past 40 ka of the core, whereas for older sections to approximately 160 ka oxygen isotope age control points were obtained by visual alignment of the δ^{18}O stratigraphy of ODP 1240 to ODP 677 (Shackleton *et al.*, 1990). The ages of ODP 1240 sampled depths were obtained from linear interpolation using 'ARAND' software (Howell, 2001). The sedimentation rates of core ODP 1240 calculated from this age model are $\sim$7–18 cm ka^{-1} (Fig. 2). The sampling interval of 8 cm utilized in this study thus provides a resolution ranging between ca. 1 and 2 ka for our records.

Samples were processed for faunal analysis using the standard procedures of Imbrie and Kipp (1971). Samples were freeze-dried and at least 300 whole planktic foraminifer specimens ($>150 \,\mu m$) were picked for faunal counting and for calculating the relative abundances of faunal species. The taxonomy of planktic foraminifers follows the schemes in Parker (1962), Bè (1967) and Kipp (1976). We also follow the taxonomic categories with exclusions of two dissolution-resistant species: *Globorotalia menardii* and *G. tumida* (Mix *et al.*, 1999). A total of 26 faunal taxa were thus used in this study (Table 1) and then fauna counts were converted to relative abundances for all identified species (see Supporting information). The faunal abundance data have
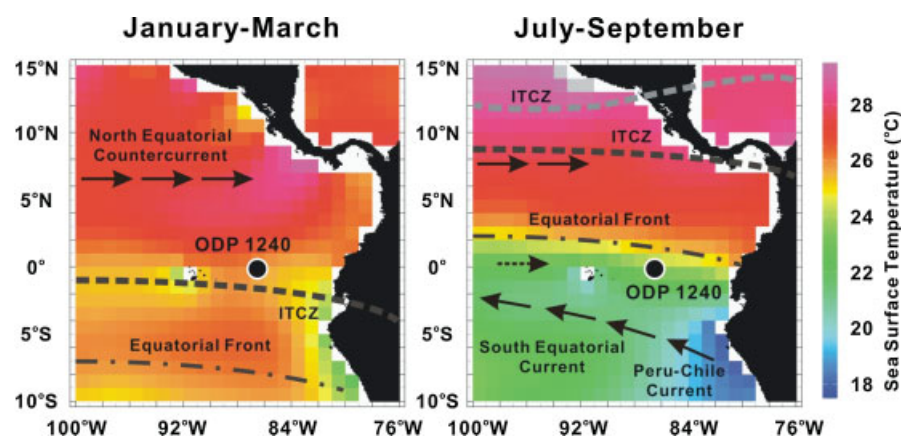

Figure 1. (a) January–March and (b) and July–September SSTs in the EEP. Prevailing surface currents (arrows) of the EP, and location of ODP Site 1240 are shown. Since ITCZ (dashed line in gray) is at its most northerly position in July–September, the PCC transports cold and nutrient-rich waters from high latitudes and results in the strongest coastal upwelling. An equatorial front that represents the northernmost mixing zone of the cold tongue in the EEP occurs in July–September.
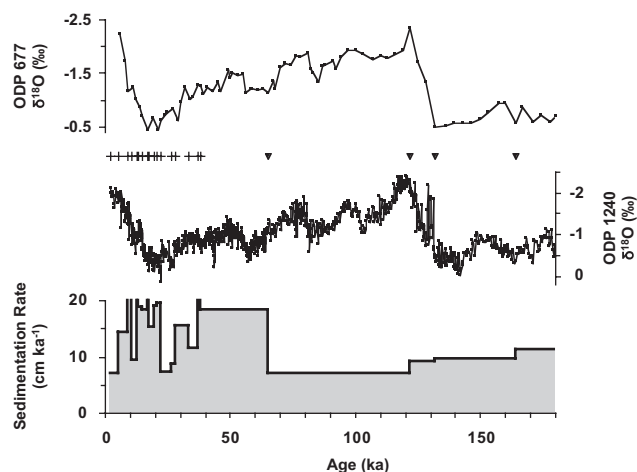
Figure 2. Age model and sedimentation rate of ODP 1240. Four age control points (shown as triangles) were obtained from correlating ODP 1240 planktic foraminifer (*G. ruber*) δ^{18}O (López-Otálvaro *et al.*, 2008) with ODP 677 (Shackleton *et al.*, 1990). AMS ^{14}C dating using planktic foraminifers from the top sections of the core are shown (crosses) (Pena *et al.*, 2008). Based on the age model, the high sedimentation rates of ODP 1240 are $\sim$7–18 cm ka^{-1}.

been log-transformed (Mix *et al.*, 1999; Feldberg and Mix, 2002) to achieve a balance of signals contained between the dominant and non-dominant species before input into a Q-mode factor analysis (VARIMAX method) (Klovan and Imbrie, 1971) (Table 1 and supporting Table S1).

IKTF SST estimation

The coretop dataset for SST calibration presented here includes 362 samples from 70° E to 140° E and from 50° N to 50° S of the

eastern Pacific (EP). In the dataset, 306 data points were taken from the MARGO database (MARGO Project Members, 2009). In order to have better data coverage for the EBC, we added 56 coretop data located along the Pacific margin of South America (20–40° S) (Mohtadi *et al.*, 2005). This new addition provides a more analogous fauna representative of the PCC water mass in our calibration dataset. Modern annual mean SSTs at 10 m water depth from WOA (1998) were assigned to each of the 362 EP coretops (hereafter EP-362) and then an SST IKTF was generated by multiple regression analysis (Imbrie and Kipp, 1971) (supporting Table S2).

Results

Coretop faunal factors

Our Q-mode factor analysis (Klovan and Imbrie, 1971) of the EP-362 coretop data shows four important faunal factors, including Equatorial, EBC, Subtropical and Subpolar faunal assemblages, that explain $\sim$87% of the total variance of the EP-362 (Table 1). Although a similarity of factor matrix and foraminifer biogeographic distribution has also been shown in previous EP studies (Feldberg and Mix, 2002), our factor matrix contains an EBC factor with much higher variance (29%, compared to 17% in Feldberg and Mix, 2002). This is not surprising, since we have added 56 new EBC coretop data into EP-362. More importantly, the faunal species *Neogloboquadrina pachyderma* (R) emerges as the single dominant species in this new EBC factor of our EP-362 (Table 1), which makes it easier to assess its ecological as well as oceanographic significance.

In our EP-362, the Equatorial and Subtropical factors account for $\sim$50% of the total variance. The Equatorial factor ($\sim$30% of the total variance) is primarily comprised of *Neogloboquadrina dutertrei* and to a lesser extent *Pulleniatina obliquiloculata*

Table 1. Q-mode factor score matrix for EP-362.

Foraminifer species	Equatorial	Subtropical	EBC	Subpolar
Orbulina universa	−0.005	0.053	0.073	0.115
Globigerinoides conglobatus	−0.002	0.140	−0.035	0.013
Globigerinoides ruber[*]	−0.101	0.572[*]	0.017	−0.111
Globoturborotalita tenella	−0.022	0.078	−0.005	0.003
Globigerinoides sacculifer[*]	0.006	0.440[*]	−0.047	−0.100
Sphaeroidinella dehiscens	0.122	0.004	−0.054	0.050
Globigerinella aequilateralis	0.068	0.252	−0.064	0.009
Globigerinella calida	0.026	0.125	0.002	−0.010
Globigerina bulloides[*]	−0.087	0.184	0.371[*]	0.463[*]
Globigerina falconensis	−0.033	0.061	0.034	0.058
Beela digitata	0.062	0.015	−0.013	0.093
Globoturborotalita rubescens	−0.013	0.053	0.003	−0.005
Turborotalita quinqueloba	−0.021	−0.033	0.071	0.268
Neogloboquadrina pachyderma (L)[*]	−0.079	−0.104	0.310[*]	0.390[*]
Neogloboquadrina pachyderma (R)[*]	−0.075	−0.062	0.800[*]	−0.385[*]
Neogloboquadrina dutertrei[*]	0.877[*]	0.009	0.234	−0.017
Globoquadrina conglomerata	0.103	0.167	−0.077	0.006
Globorotaloides hexagonus	−0.001	0.129	0.020	−0.006
Pulleniatina obliquiloculata[*]	0.401[*]	0.097	−0.143	0.085
Globorotalia inflate[*]	0.011	−0.040	0.032	0.446[*]
Globorotalia truncatulinoides (L)	−0.012	0.009	0.028	0.035
Globorotalia truncatulinoides (R)[*]	0.016	−0.023	−0.067	0.361[*]
Globorotalia crassaformis	0.028	0.002	−0.005	0.109
Globorotalia hirsuta	−0.004	0.018	−0.001	0.002
Globorotalia scitula	−0.024	0.044	0.040	0.071
Globigerinita glutinata[*]	−0.041	0.507[*]	0.123	0.094
Variance (%)	29.729	20.240	29.109	7.893
Cumulative variance (%)	29.729	49.969	79.078	86.970

[*] Asterisks indicate dominant species (factor scores < -0.3 and/or >0.3).

(Table 1). The coretops with high Equatorial factor loadings are commonly distributed in warm equatorial waters, especially in most tropical regions (10° N–10° S, west of 100° W; Fig. 3a). A gradual decrease of the Equatorial factor from the central equatorial Pacific to the Panama Basin reflects interactions between warm water from the west and cool water masses from the high latitudes. Moderate highs of the factor can be found in the California Current and PCC regions, where the increased *N. dutertrei* abundances are indicative of a more nutrient-rich

water supply from the coastal upwelling zones (supporting Fig. S1a). The Subtropical factor (∼20% of the total variance; Table 1), which is comprised of *G. ruber*, *Globigerinoides sacculifer* and *Globigerinita glutinata*, is most dominant in the oligotrophic equatorial water and the subtropical gyre (∼10–20° S), while a secondary maximum is observed in the eastern equatorial warm pool (Fig. 3b).

The EBC and Subpolar factors represent 29% and 8% of the total variances of the EP-362 dataset, respectively. The EBC
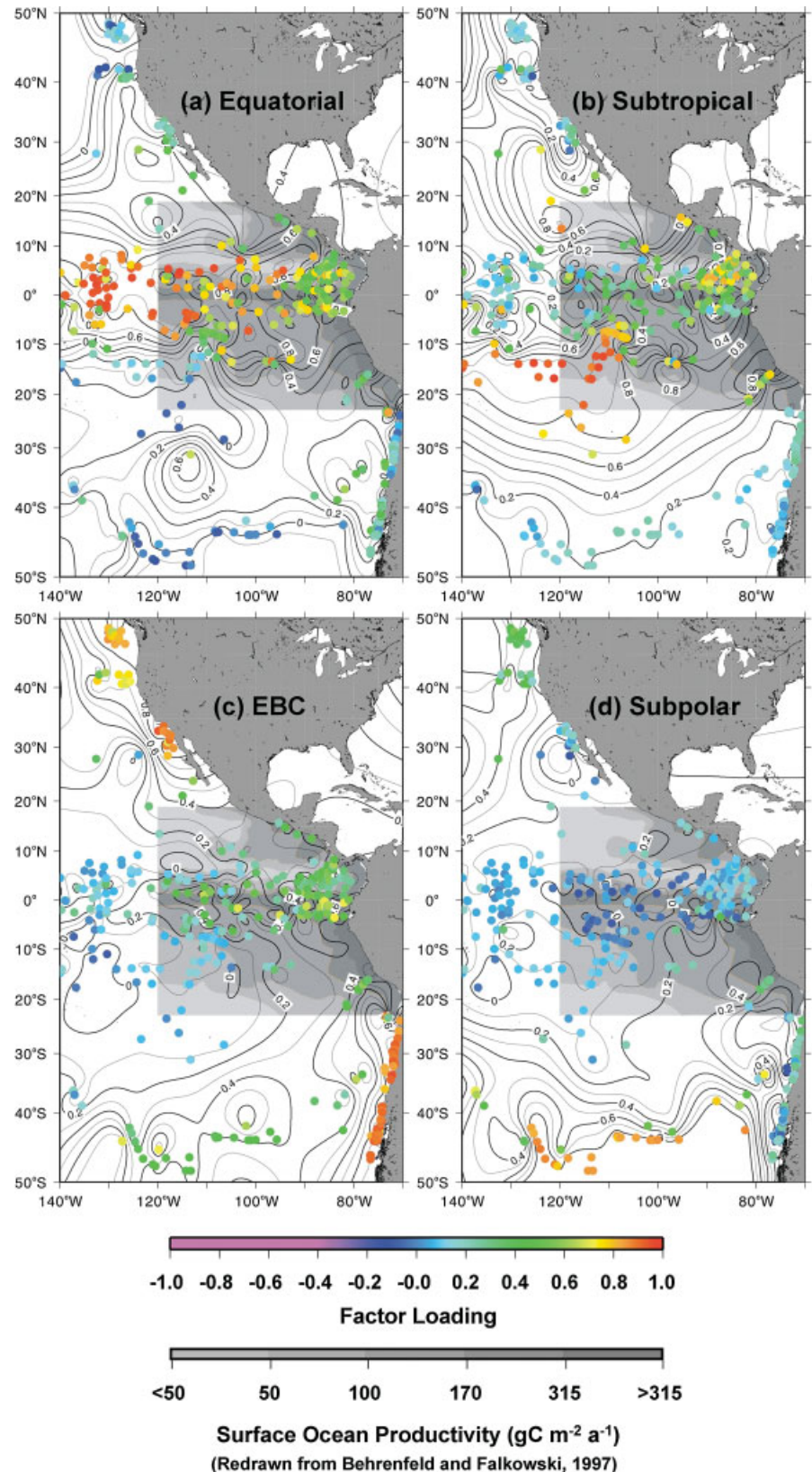

Figure 3. Spatial distributions of (a) Equatorial, (b) Subtropical, (c) EBC and (d) Subpolar faunal factor loading, decomposed from the EP-362 coretop calibration dataset (Table 1). Modern surface ocean productivity (g carbon m^{-2} a^{-1}) in the EEP (redrawn from Behrenfeld and Falkowski, 1997) is shown in gray scale in the EEP (20° N–20° S, 120° W–70° W).

factor is dominated by *N. pachyderma* (R), and is also related to *Globigerina bulloides* and *N. pachyderma* (L), whereas four species contribute equally to the Subpolar factor: *G. bulloides*, *Globorotalia inflata*, *N. pachyderma* (L) and *Globorotalia truncatulinoides* (R) (Table 1). The EBC factor is high in coastal upwelling zones of the California Current and PCC (Fig. 3c), mimicked by the spatial distribution of *G. bulloides* and *N. pachyderma* (R) abundance patterns (supporting Fig. S1b,d). In the southeastern Pacific sector parallel to a zone near 40–50°S (Fig. 3d) the Subpolar factor is high, which indicates the co-occurrence of the four species related to the factor (Table 1), in particular *G. inflata* and *G. bulloides* (supporting Fig. S1d,f).

Downcore faunal factor variations: implications of water mass exchanges

The four factors delineated above explain the downcore faunal variations at site ODP 1240 very well, as evidenced by the high communalities always exceeding 0.8 (supporting Fig. S2). The Equatorial factor is relatively high during MIS 1, 5, 6 and low during MIS 2 and the MIS 3/4 and 5/6 transitions (Fig. 4). The EBC factor shows maxima during MIS 2 and early MIS 3, and exhibits minima during MIS 1 and late MIS 3, and is very low during the MIS 5/6 transition (Fig. 4). Together, this indicates that the faunal variations do not follow strictly glacial and interglacial stages. It is also noted that the Subtropical and Equatorial factors share a similar pattern of variation in the younger part (MIS 1–4), but become anti-phased in the older part of the record (MIS 5–6), thus implying fundamentally different oceanographic conditions at site 1240 during these two time intervals. At MIS 6, the Subpolar factor (*G. bulloides* dominated) is in parallel with the Subtropical factor, reflecting

Figure 4. Variations in ODP 1240 Equatorial, Subtropical, EBC and Subpolar faunal factors and estimated SSTs (IKTF estimates excluding *G. menardii* + *G. tumida* in blue; and IKTF estimates including *G. menardii* + *G. tumida* in gray) of the past 160 ka, plotted against ODP 1240 δ¹⁸O (Pena *et al.*, 2008). Shaded intervals indicate glacial MIS. This figure is available in colour online at wileyonlinelibrary.com/journal/jqs.

stronger intrusion of high-latitude subpolar water masses into the Subtropics. At the same time, the reduced EBC (*N. pachyderma* (R)) and Equatorial (nutrient-related *N. dutertrei*) factors imply weakened/less extended cool, nutrient-rich PCC/coastal upwelling waters. From MIS 5/6 transition to ca. 110 ka, the vigorous EBC advection begins to replace the subpolar component, while the subtropical component remained nearly constant. Notable minima in EBC loadings around MIS 5/6 transition imply weakened EBC advection/coastal upwelling waters; however, two lowest EBC loadings ca. 115 ka are possibly related to poor carbonate preservation of *N. pachyderma* (R).

During MIS 2 to late MIS 3, pronounced reductions in the Equatorial and Subtropical factors, along with the maxima of the Subpolar factor, suggest a shrinkage of equatorial warm water and simultaneously reduced coastal upwelling, with a strengthened intrusion of cold water from high-latitude subpolar regions at that time. The increased Subpolar influences correlate well with the cooling maxima of ∼3–5°C (relative to coretop values) during MIS 2 to late MIS 3 (ca. 18–36 ka). It is interesting to note that although the EBC factor is also high during MIS 2, the EBC is not as high during late MIS 3, implying that the EBC is not the sole factor responsible for low SSTs. Another instance indicating the linkage of increased Subpolar influence to reduced SSTs is evident at the MIS 3/4 transition (ca. 58–60 ka), and during a short episode during late MIS 5 (ca. 76–78 ka). Based on the observed coincidence of faunal changes and SST variations, we suggest that the major cooling intervals observed at ODP 1240 are more closely linked to the intrusion of southern subpolar water masses than to equatorial or coastal upwelling.

Downcore estimated SSTs

Our IKTF SST estimates for ODP 1240 indicate higher SSTs during interglacial and lower SSTs during glacial periods (Fig. 4). Maximum cooling of ∼3–5°C occurred during the MIS 2 to late MIS 3 time interval and during the MIS 3/4 transition, whereas faunal SSTs during most of MIS 5–6 fluctuated only by ∼1–2°C, which is smaller than the Mg/Ca SST records of ODP 1240 (∼3–4°C; Pena *et al.*, 2008). This small amplitude of IKTF SST variation appears not to be an artifact driven by differential preservation of faunal samples, as our foraminifer fragmentation data (see supplementary information) show a typical 'Pacific-type' carbonate dissolution cycle, which is nearly stationary during MIS 1–6. It is also noted, that though temperature of glacial MIS 6 (23.8 ± 0.5°C) is close to the modern (WOA, 2009; Locarnini *et al.*, 2010) (Fig. 4), warm- and cold-water mass exchanges in MIS 6 have dramatic variations, as evidenced by downcore faunal factors (see previous subsection).

Our faunal data imply an expansion of subtropical gyre waters into the EEP from the MIS 5/6 transition until the end of MIS 5.5. The SSTs during MIS 5.5 (∼26°C) are similar to those in the late Holocene, in agreement with previous estimates based on radiolarian faunas (Pisias and Mix, 1997), Mg/Ca (Lea *et al.*, 2002) and $U^{K'}_{37}$ (Liu *et al.*, 2008) around the Galapagos area. However, the faunal assemblages provide additional causal constraints on SST variability. Thus the surface water in the EEP during MIS 5.5 remained subtropical warm water, whereas after MIS 5.5 the surface waters at ODP 1240 were influenced by the EBC and subpolar water masses. A short-lived cooling of ∼2°C during late MIS 5 (ca. 76–78 ka) was caused by a sudden increase in the relative abundance of *G. inflata* (see supporting information) – one of the indicators of a subpolar water mass.

A major cooling (∼4–5°C, relative to the coretop value) during late MIS 4 is comparable to that of the LGM (Fig. 4). The
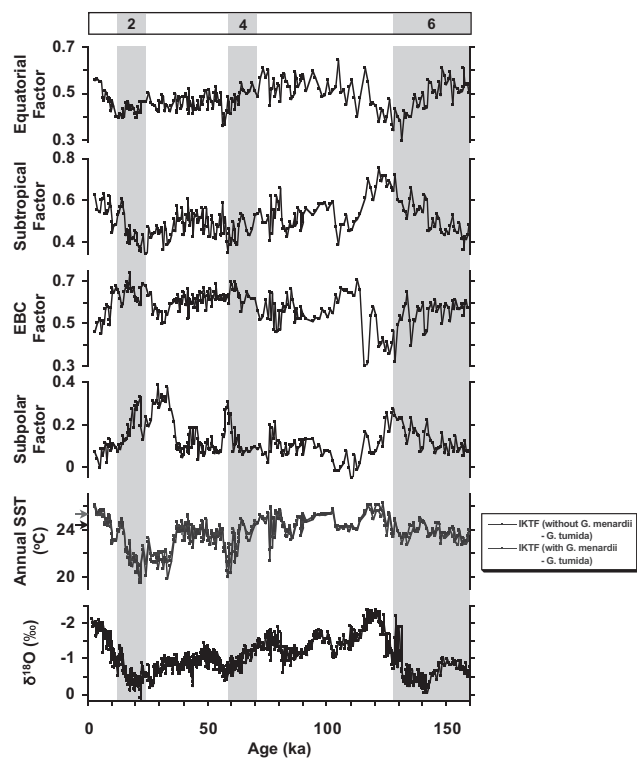
long-term cooling trend in our IKTF SST record of ODP 1240 since MIS 5 has been exacerbated by even stronger millennial-scale cooling of up to ~2–5°C (e.g. ca. 76–78, 58–60 and 18–36 ka). Among the series of strong cooling events, the most pronounced one at ca. 36–18 ka is not observed in the alkenone SST record of core ME0005-24JC near our location (Kienast *et al.*, 2006) or in the Mg/Ca SST records of ODP 1240 (Pena *et al.*, 2008). However, the very strong millennial-scale cooling shown in our IKTF SST appears to be a common feature in other fauna-based estimates (Pisias and Mix, 1997; Feldberg and Mix, 2002, 2003), indicating a major discrepancy between the faunal and geochemical results of EEP SST estimates. Moreover, our IKTF SST estimates show an average

SST of 20.8°C during the LGM (23–19 ka), which is ~5°C lower than the late Holocene (4–0 ka) or ~3–4°C lower than modern (Locarnini *et al.*, 2010). The magnitude of LGM cooling (i.e. LGM minus WOA98) at site 1240 is consistent with previous LGM faunal SST reconstructions for the LGM derived from regional EP or entire Pacific calibrations (~3–5°C; Feldberg and Mix, 2002; MARGO Project Members, 2009), but is greater than alkenone SST (Kienast *et al.*, 2006) and Mg/Ca SST (Pena *et al.*, 2008) LGM estimates, which indicate a cooling of only ~2–3°C. The discrepancies among different SST reconstructions could be ascribed to the different sensitivities of these SST methodologies themselves, and/or different optimum growing seasons of planktic foraminifer or coccolithopore species
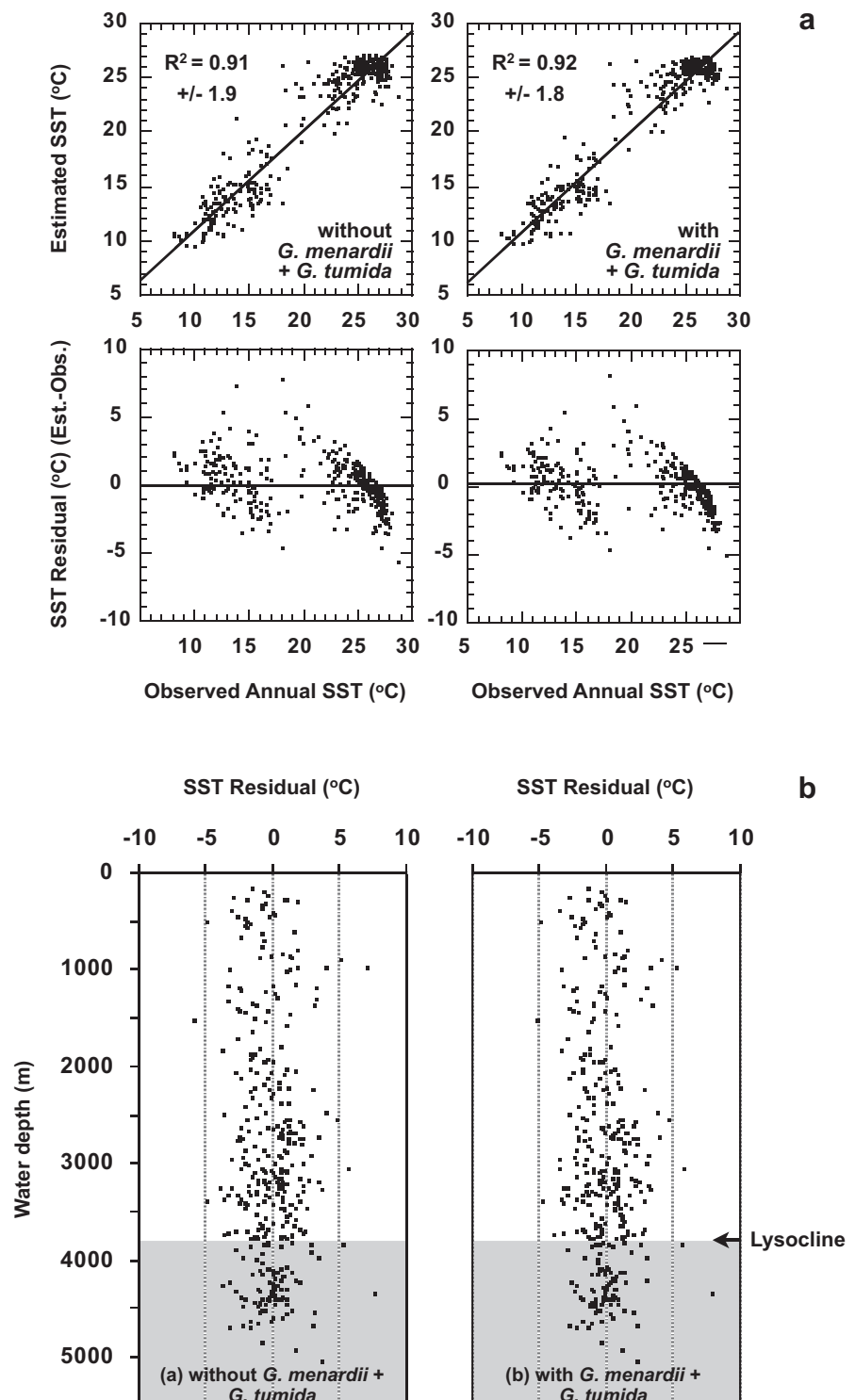

Figure 5. (a) Scatter-plots for observed and estimated IKTF SSTs (with or without *G. menardii* + *G. tumida*) and for observed IKTF SSTs and SST residuals (estimated minus observed) (without or with *G. menardii* + *G. tumida*). (b) Plots for SST residuals against water depths of EP-362 coretops. Shaded areas indicate that coretop depths are under a regional carbonate lysocline of ~3800 m. (c) Spatial distributions of SST residuals (without or with *G. menardii* + *G. tumida*).

(Nürnberg *et al.*, 2000; Bard, 2001). We note that the strong cooling at 18–36 ka corresponds to the sudden increase in *G. inflata* abundances (see supporting information) representative of a subpolar water mass. Our data thus imply an oceanographic mechanism in bringing subpolar cooling from the Extratropics to the EEP during the millennial-scale cooling events (e.g. ca. 76–78, 58–60 and 18–36 ka), to which other geochemical proxies might be insensitive or beyond the dynamic range.

Discussion

Assessment of EP-362 coretop calibrations

Our faunal analysis presented here suggests that four factors are needed to characterize the faunal assemblages with the water masses in which the faunas were living in the EP (Feldberg and Mix, 2002). However, by adding more coretop data from the PCC (Mohtadi *et al.*, 2005), the variance in our EBC factor is increased (Table 1 and supporting Table S1). More importantly, our factor matrix identifies *N. pachyderma* (R) as the most dominant species in the EBC factor, which has not been clearly shown in previous studies (supporting Table S1). Overall, the new EP-362 data provide an avenue for better defining faunal assemblages of the EBC and Subpolar in the EP, and also improve on the 'no-analogue' problem encountered in previous studies (Feldberg and Mix, 2002).

Furthermore, our IKTF was developed based on four faunal factors derived from EP-362. While testing the IKTF against the EP-362 coretop data (Fig. 5a), we found good agreement between estimated SST values and observed SSTs ($r^2 = 0.91$; RMS = 1.9). We assessed potential SST biases associated with differential preservation by establishing the IKTFs with/without *G. menardii* + *G. tumida* species, but found no significant difference between the two estimations for the coretop (Fig. 5a) or downcore data (Fig. 4). The SST residuals (estimated minus observed SSTs) are independent of water depth in either case (Fig. 5b), implying that our IKTF SST estimates are insensitive to differential preservation of faunal samples. While assessing the SST residual on a spatial scale (Fig. 5c), we found that the biases of our SST estimates are regionally independent, though some SSTs are slightly underestimated (< -2°C) in the western EP and in the Panama Basin, and overestimated (>2°C) in the East Pacific Rise area of the EP and in some coastal upwelling zones (Fig. 5b).

The sensitivity of our IKTF is subject to controls by hydrographic conditions other than SST (Morey *et al.*, 2005). For example, hydrographic conditions in the Panama Basin are characterized by a year-round and profound warm-pool condition with high precipitation (>150 cm a^{-1}), low SSS (<33), a shallow pycnocline ($\sim$60 m) and relatively low productivity in the upper water column (Fiedler and Talley, 2006). The distinctive hydrographic conditions may modify the habitat of the plankton community and/or the faunal composition, and therefore may indirectly affect SST estimates in this region (Pisias and Mix, 1997; Mix *et al.*, 1999). Nevertheless, we consider that the biases are limited to a small spatial scale and are not substantial enough to change the downcore pattern of our SST estimates for ODP 1240 in particular.

EEP oceanographic reconstruction since MIS 6

With the new IKTF, we are able to assess past cold tongue variability since MIS 6 on a more spatial scale. These new faunal records and implied water mass changes also provide direct constraints on upper water column structure in the EEP in previous studies (e.g. Spero *et al.*, 2003; Dubois *et al.*, 2009). To reach this goal, we have compiled planktic foraminifer faunal records with published age models (Chen, 1994; McKenna *et al.*, 1995; Mix *et al.*, 1999) from the EEP (10° N–20° S, 120–70° W) (Fig. 6a), and then decomposed the EEP faunal records

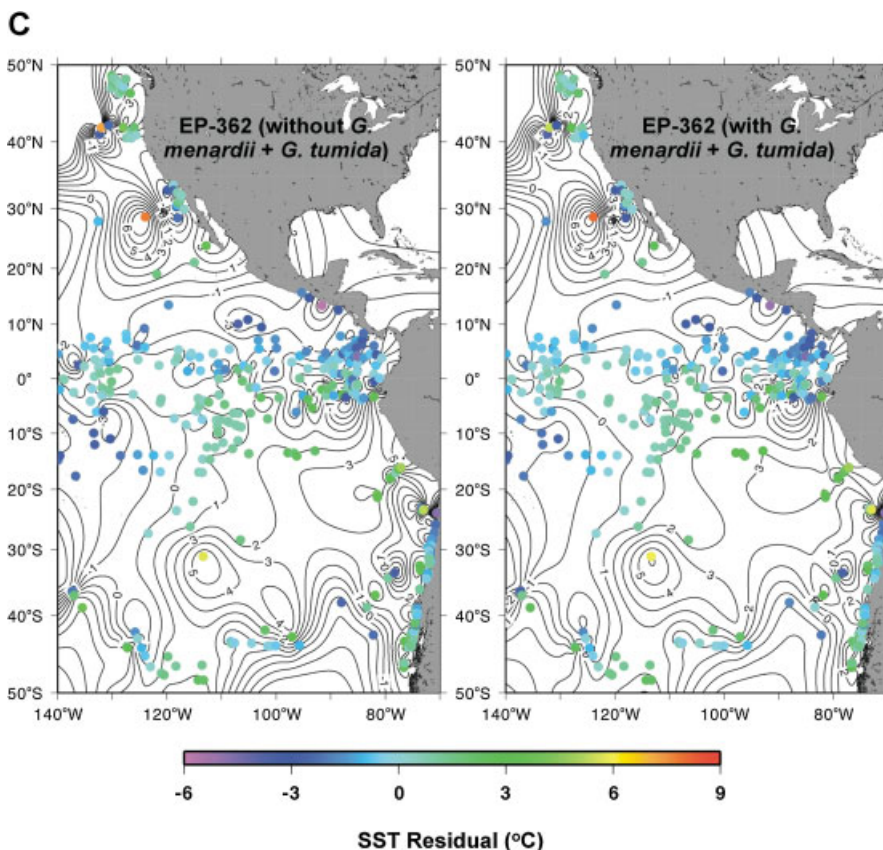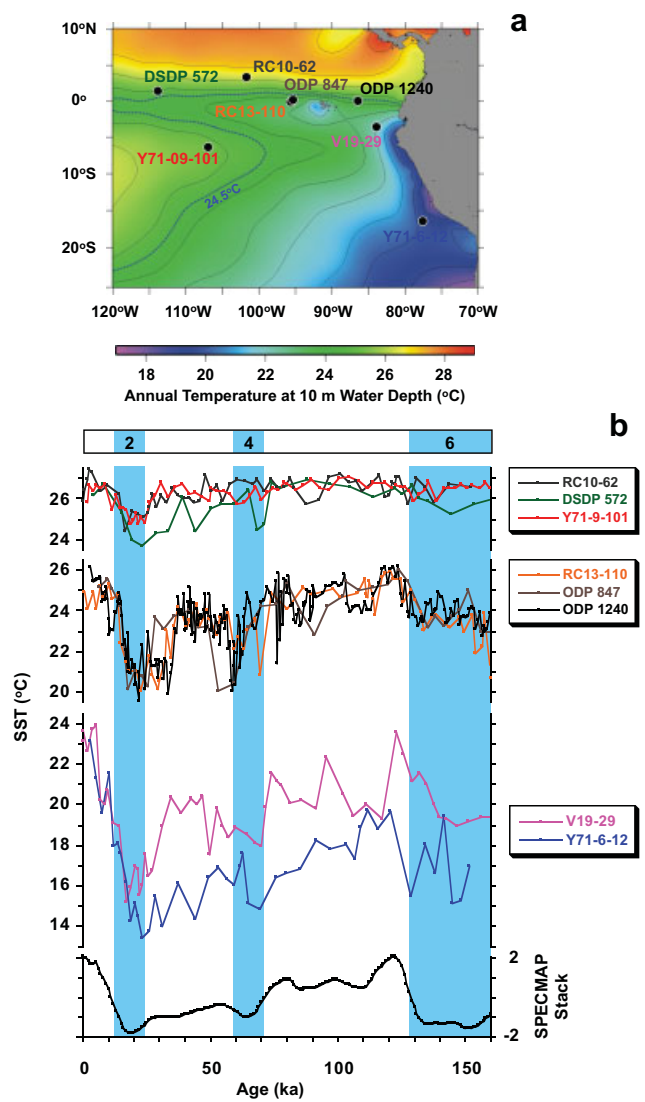**Figure 5.** (*Continued*)

Figure 6. (a) A map showing the locations of the faunal records from the EEP (Chen, 1994; McKenna *et al.*, 1995; Mix *et al.*, 1999; ODP 1240, this study). (b) SST estimates by IKTF based on EP-362. Three groups from top to bottom: 'warm water margin'; 'central cold tongue'; and 'coastal upwelling zone'. SSTs are plotted against age; shaded intervals indicate glacial MIS.

into factors and calculated estimates of SSTs (Fig. 6b). For convenience, these records are divided into three groups based on their modern locations: (i) the 'warm water margin' (RC10-62, DSDP572, Y71-9-101); (ii) the 'central cold tongue' (RC13-110, ODP 847, ODP 1240); and (iii) the 'coastal upwelling zone' (V19-29, Y71-6-12). Examining the spatial patterns shown in these records is difficult, as the age models of these records have been developed independently, and changes in sedimentation rate and sampling intervals of the cores have made analysis at the same resolution impossible. Despite these difficulties, one striking feature emerges from our observations: both 'warm water margin' and 'central cold tongue' groups show a long-term cooling trend since MIS 6. The northern record (V19-29) from the 'coastal upwelling zone' group shows a relatively weak trend of such long-term cooling. The long-term cooling trend is exacerbated by several very strong millennial-scale cooling events since MIS 6. Most of the cooling events happened during the MIS 4/5 or 3/4 transitions, and during late MIS 3 to MIS 2. It is impossible to constrain whether or not these cooling events are synchronous because the individual age model have an uncertainty of several thousand years (Table 2).
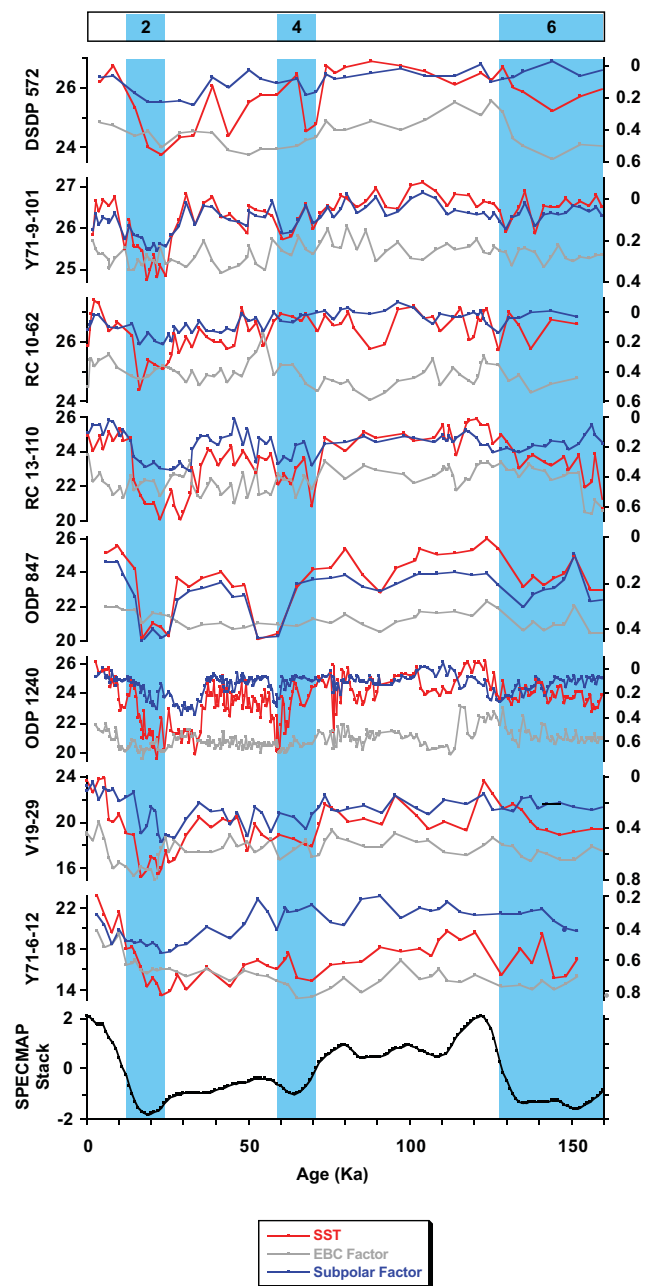

Figure 7. IKTF SST estimates, EBC and Subpolar factors of faunal records shown in Figure 6, plotted against age. Shaded intervals indicate glacial MIS.

Another noticeable feature is that the variations of Subpolar factors parallel quite closely the estimated SSTs, in which more dominant subpolar faunal assemblages are linked with low SSTs (Fig. 7). The linkage appears to be relatively weak in the westernmost (DSDP 572) and southernmost (Y71-6-12) records of the EEP, but is strong in most other records of the EEP. This implies that the expansion or intrusion of subpolar water mass to the EEP has dominated the SST variability in the cold tongue since MIS 6. Our results differ from previous reports that an increased EBC contributes most of the glacial cooling in the EEP (Andreasen and Ravelo, 1997; Feldberg and Mix, 2002), but emphasizes that the subpolar water mass may play a more dynamic role in driving hydrographic changes in the EEP. Our finding also agrees with stable isotope records on multi-species, which suggests that the hydrography of the EEP may partly be modulated by increased advection of intermediate waters from the Antarctic polar front (Spero *et al.*, 2003).

Table 2. Age models and resolutions (0–150 ka) of faunal records from the EEP.

Core ID	Age model	Average resolution (ka)	Reference
DSDP 572	*G. sacculifer*	5.4	Farrell and Prell (1991)
ODP 847	*G. sacculifer, N. dutertrei*	4.3	Farrell *et al.* (1995)
ODP 1240	*G. ruber*	0.7	This study
RC10-62	*N. dutertrei*	2.5	Pisias and Mix (1997)
RC13-110	Benthic foraminifers	2.2	Pisias and Mix (1997)
V19-29	Benthic foraminifers	2.8	Pisias and Mix (1997)
Y71-6-12	*N. dutertrei*	3.6	Pisias and Mix (1997)
Y71-9-101	*N. dutertrei*	2.2	Pisias and Mix (1997)

'Coastal upwelling zone' records reveal that the EBC and subpolar water masses have fluctuated dynamically since MIS 6 (Fig. 6b). The southern record Y71-6-12 receives direct influence from EBC/subpolar cold waters advected from mid latitudes and experiences a substantial cooling of ~8–9°C during late MIS 3 to MIS 2 and a cooling of ~4–5°C during the MIS 4/5 transition. Located at the mixing zone of the EBC and cold tongue water, V19-29 experiences ~8–9°C during late MIS 3 to MIS 2 and two cooling episodes of ~2–4°C during the MIS 4/5 and MIS 3/4 transitions. The millennial-scale SST variations shown in the 'coastal upwelling zone' group are significantly larger than the other two groups, suggesting that the water advected from the coastal upwelling zone or even from southern high latitudes have driven the SST variability in the EEP.

Although our faunal studies provide evidence that the subpolar water mass has been a major dynamic contributor to EEP cold tongue cooling since MIS 6, the pathways by which the subpolar water entrain or intrude into the EEP are not identifiable from the faunal evidence. Modern cold tongue water could be supplied from: (i) advection of the PCC waters driven by westerlies (Wyrtki, 1981); (ii) northward transported EBC/subpolar water via the PCC (Wyrtki, 1981); (iii) ventilated subpolar water along the mid-latitude gyre (Harper, 2000); and/ or (iv) the eastward subsurface transport of EUC water originating from the Subantarctic Mode Water (Toggweiler *et al.*, 1991). Identification of these 'pathways' will require studies using geochemical or other isotope tracers for the past oceans, which are beyond the scope of this study.

While complicated by strong mixing of different water masses and the varied resolution of faunal SST records with age uncertainties, our EEP dataset suggests the intensity and geometry of the EEP cold tongue have changed over time since MIS 6. The cold tongue may have intensified and expanded greatly to the north and west during early MIS 2, as revealed by very strong surface cooling shown in the 'central cold tongue' records and strong cooling in the 'warm water margin' records (Fig. 6b). The intensified cold tongue may have migrated slightly to the south during late MIS 3, as the same strong cooling is shown in 'central cold tongue' records, while the 'warm water margin' group shows a warming. The same cold tongue geometry appears to have occurred during the MIS 3/4 transition. The complex intensity and geometric changes in part explain why a single record of the EEP always shows spiky signals that are unparalleled in global glacial and interglacial climates. However, from records related to spatial parameters, we conclude that the variability of cold tongue SST is governed mainly by the dynamics of subpolar water masses, but the intensity and geometry of the cold tongue have been governed by additional mechanisms, which will need to be included to better understand the spatial variability of the cold tongue in the EEP.

Conclusions

We develop an IKTF based on a coretop calibration dataset (EP-362) that is supplemented by more data from the PCC, and use it to estimate SSTs from planktic foraminifer faunal assemblages of the EEP. A Q-mode factor analysis is used to decompose the faunal assemblage data into Equatorial, EBC, Subtropical and Subpolar factors, and provides well-defined EBC and Subpolar factors. The IKTF is demonstrated to better address problems of 'no-analogue' faunas and differential preservation of faunal assemblages in estimating SSTs for the EEP. In applying the IKTF to faunal records of ODP 1240, we found that two substantial cooling intervals (~4–5°C, relative to the coretop value of ODP 1240) occurred during the late MIS 3 to MIS 2 and late MIS 4. A minor, shorted-lived cooling of ~2°C occurred during late MIS 5. The ODP 1240 SST record shows a long-term cooling trend since MIS 6. The long-term cooling has been exacerbated by even stronger millennial-scale cooling of up to ~2–5°C. The strong cooling shown in our ODP 1240 record corresponds to an increase in the Subpolar factor, suggesting that the subpolar water mass contributed to cooling in the EEP. By applying the IKTF to faunal records from seven sites in the EEP, we find that both the intensity and geometry of the cold tongue in the EEP have been highly dynamic since MIS 6, and the intrusions of subpolar water from high latitudes and other mechanisms must be taken into account in order to explain the variability.

Supporting information

Additional supporting information can be found in the online version of this article:

Fig. S1. Abundance distributions of dominant coretop planktic foraminifer species in the EEP.

Fig. S2. Downcore abundance variations of dominant planktic foraminifer species in ODP 1240.

Table S1 Q-mode factor score matrix.

Table S2 Multivariate regression coefficients.

Table S3 The means, standard deviations, minima, and maxima of planktic foraminifer faunal abundances in ODP 1240.

Please note: This supporting information is supplied by the authors, and may be re-organized for online delivery, but is not copy-edited or typeset by Wiley-Blackwell. Technical support issues arising from supporting information (other than missing files) should be addressed to the authors.

Abbreviations. EBC, eastern boundary current; EEP, eastern equatorial Pacific; EP, eastern Pacific; EUC, equatorial undercurrent; IKTF, Imbrie–Kipp transfer function; ITCZ, intertropical convergence zone; LGM, Last Glacial Maximum; MIS, Marine Isotope Stage; NADW, north Atlantic deep water; PCC, Peru–Chile Current; SST, sea surface temperature.

References

Amador JA, Alfaro EJ, Lizano OG, *et al.* 2006. Atmospheric forcing of the eastern tropical Pacific: a review. *Progress in Oceanography* **69**: 101–142.

Andreasen DJ, Ravelo AC. 1997. Tropical Pacific Ocean thermocline depth reconstructions for the last glacial maximum. *Paleoceanography* **12**: 395–413.

Bard E. 2001. Comparison of alkenone estimates with other paleotemperature proxies. *Geochemistry, Geophysics, Geosystems* **2**: 1002.

Bè AWH. 1967. Foraminifera, families: Globigerinidae and Globorotaliidae. In *Fiches d'Identification du Zooplancton*, Fraser JH (ed.). International Council for the Exploration of the Sea: Charlottenlund; Sheet 108.

Behrenfeld M, Falkowski P. 1997. Photosynthetic rates derived from satellite based chlorophyll concentration. *Limnology and Oceanography* **42**: 1–20.

Benway HM, Mix AC, Haley BA, *et al.* 2006. Eastern Pacific Warm Pool paleosalinity and climate variability:0-30 kyr. *Paleoceanography* **21**: PA3008.

Cane M, Clement AC. 1999. A role of the tropical Pacific coupled ocean–atmosphere system on Milankovitch and millennial time-scales: 2. Global impacts. In *Mechanisms of Global Climate Change at Millennial Time-Scales*, Clark PU, Webb RS, Keigwin LD (eds). Geophysical Monograph Series Vol. 112 AGU: Washington, DC; 373–383.

Chen M-T. 1994. Late quaternary paleoceanography of the equatorial Indo-Pacific Ocean: a quantitative analysis based on marine micropaleontological data. PhD thesis, Brown University.

Chiang JCH. 2009. The Tropics in paleoclimate. In *Annual Review of Earth and Planetary Sciences*, Vol. 37, Jeanloz R, Freeman KH (eds). Annual Reviews: Palo Alto: CA; 263–297.

Clement AC, Peterson LC. 2008. Mechanisms of abrupt climate change of the last glacial period. *Reviews of Geophysics* **46**: RG4002.

Dubois N, Kienast M, Normandeau C, *et al.* 2009. Eastern equatorial Pacific cold tongue during the Last Glacial Maximum as seen from alkenone paleothermometry. *Paleoceanography* **24**: PA4207.

Farrell JW, Prell WL. 1991. Pacific CaCO$_3$ preservation and δ^{18}O since 4 Ma: paleoceanic and paleoclimatic implications. *Paleoceanography* **6**: 485–498.

Farrell JW, Murray DW, McKenna VS, *et al.* 1995. Upper ocean temperature and nutrient contrasts inferred from Pleistocene planktonic foraminifer δ^{18}O and δ^{13}C in the eastern equatorial Pacific. In *Proceedings of the Ocean Drilling Program, Scientific Results*, Vol. 138, Pisias NG, Mayer LA, Janecek TR, Palmer-Julson A, van Andel TH (eds). Ocean Drilling Program: College Station, TX; 289–319.

Feldberg MJ, Mix AC. 2002. Sea-surface temperature estimates in the Southeast Pacific based on planktonic foraminiferal species: modern calibration and Last Glacial Maximum. *Marine Micropaleontology* **44**: 1–29.

Feldberg MJ, Mix AC. 2003. Planktonic foraminifera, sea surface temperatures, and mechanisms of oceanic change in the Peru and south equatorial currents, 0-150 ka BP. *Paleoceanography* **18**: 1016.

Fiedler PC, Talley LD. 2006. Hydrography of the eastern tropical Pacific: a review. *Progress in Oceanography* **69**: 143–180.

Harper S. 2000. Thermocline ventilation and pathways of tropical–subtropical water mass exchange. *Tellus* **52A**: 330–345.

Howell P. 2001. *ARAND time series and spectral analysis package for the Macintosh.* Brown University: Providence, RI.

Imbrie J, Kipp NG. 1971. A new micropaleontological method for quantitative paleoclimatology: application to a Late Pleistocene Caribbean core. In *The Late Cenozoic Glacial Ages*, Turekian KK (ed.). Yale University Press: New Haven, CT; 71–181.

Kienast M, Kienast SS, Calvert SE, *et al.* 2006. Eastern Pacific cooling and Atlantic overturning circulation during the last deglaciation. *Nature* **443**: 846–849.

Kipp NG. 1976. New transfer function for estimating past sea-surface conditions from sea-bed distribution of planktonic foraminiferal assemblages in the North Atlantic. *Geological Society of America Memoir* **145**: 3–41.

Klovan JE, Imbrie J. 1971. An algorithm and FORTRAN-IV program for large scale Q-mode factor analysis and calculation of factor scores. *Journal of Mathematical Geology* **3**: 61–76.

Koutavas A, Lynch-Stieglitz J. 2003. Glacial–interglacial dynamics of the eastern equatorial Pacific cold tongue–Intertropical Convergence Zone system reconstructed from oxygen isotope records. *Paleoceanography* **18**: 1089.

Lea DW, Pak DK, Spero HJ. 2000. Climate impact of late Quaternary equatorial Pacific sea surface temperature variations. *Science* **289**: 1719–1724.

Lea DW, Martin PA, Pak DK, *et al.* 2002. Reconstructing a 350 ky history of sea level using planktonic Mg/Ca and oxygen isotope records from a Cocos Ridge core. *Quaternary Science Reviews* **21**: 283–293.

Leduc G, Vidal L, Tachikawa K, *et al.* 2007. Moisture transport across central America as a positive feedback on abrupt climatic changes. *Nature* **445**: 908–911.

Liu Z, Cleaveland LC, Herbert TD. 2008. Early onset and origin of 100-kyr cycles in Pleistocene tropical SST records. *Earth and Planetary Science Letters* **265**: 703–715.

Locarnini RA, Mishonov AV, Antonov JI, *et al.* 2010. World Ocean Atlas. 2009, Vol. 1: *Temperature*, Levitus S (ed.). NOAA Atlas NESDIS 68, US Government Printing Office: Washington, DC; 1–184.

López-Otálvaro GE, Flores JA, Sierro FJ, *et al.* 2008. Variations in coccolithophorid production in the Eastern Equatorial Pacific at ODP Site 1240 over the last seven glacial-interglacial cycles. *Marine Micropaleontology* **69**: 52–69.

MARGO Project Members. 2009. Constraints on the magnitude and patterns of ocean cooling at the Last Glacial Maximum. *Nature Geoscience* **2**: 127–132.

Martínez I, Keigwin L, Barrows TT, *et al.* 2003. La Niña-like conditions in the eastern equatorial Pacific and a stronger Choco jet in the northern Andes during the last glaciation. *Paleoceanography* **18**: 1033.

Martinez I, Rincon D, Yokoyama Y, *et al.* 2006. Foraminifera and coccolithophorid assemblage changes in the Panama Basin during the last deglaciation: response to sea-surface productivity induced by a transient climate change. *Palaeogeography, Palaeoclimatology, Palaeoecology* **234**: 114–126.

Martínez-Garcia A, Rosell-Melé A, McClymont EL, *et al.* 2010. Sub-polar link to the emergence of the modern equatorial Pacific cold tongue. *Science* **328**: 1550–1553.

McKenna VS, Farrell JW, Murray DW, *et al.* 1995. The foraminifer record at Site 847: paleoceanographic response to late Pleistocene climate variability. In *Proceedings of the Ocean Drilling Program, Scientific Results*, Vol. 138, Pisias NG, Mayer LA, Janecek TR, Palmer-Julson A, van Andel TH (eds). Ocean Drilling Program: College Station, TX; 695–714.

Mix AC, Morey AE, Pisias NG, *et al.* 1999. Foraminiferal faunal estimates of paleotemperature: circumventing the no-analog problem yields cool ice-age tropics. *Paleoceanography* **14**: 350–359.

Mix AC, Tiedemann R, Blum P. Shipboard Scientific Party. 2003. *Proceedings of the Ocean Drilling Program Initial Reports*, Vol. **202**

Mohtadi M, Hebbeln D, Marchant M. 2005. Upwelling and productivity along the Peru–Chile Current derived from faunal and isotopic compositions of planktic foraminifera in surface sediments. *Marine Geology* **216**: 107–126.

Morey AE, Mix AC, Pisias NG. 2005. Planktonic foraminiferal assemblages preserved in surface sediments correspond to multiple environment variables. *Quaternary Science Reviews* **24**: 925–950.

Nürnberg D, Müller A, Schneider RR. 2000. Paleo-sea surface temperature calculations in the equatorial east Atlantic from Mg/Ca ratios in planktic foraminifera: a comparison to sea surface temperature estimates from U$^{K'}_{37}$, oxygen isotopes, and foraminiferal transfer function. *Paleoceanography* **15**: 124–134.

Pak H, Zaneveld JRV. 1974. Equatorial front in the eastern equatorial Pacific Ocean. *Journal of Physical Oceanography* **4**: 570–578.

Parker FL. 1962. Planktonic foraminiferal species in Pacific sediments. *Micropaleontology* **8**: 219–254.

Pena LD, Cacho I, Ferretti P, *et al.* 2008. ENSO-like variability during glacial terminations and interlatitudinal tele-connections. *Paleoceanography* **23**: PA3101.

Pennington JT, Mahoney KL, Kuwahara VS, *et al.* 2006. Primary production in the eastern tropical Pacific: a review. *Progress in Oceanography* **69**: 285–317.

Pisias NG, Mix AC. 1997. Spatial and temporal oceanographic variability of the eastern equatorial Pacific during the late Pleistocene: evidence from radiolarian microfossils. *Paleoceanography* **12**: 381–393.

Prahl FG, Mix AC, Sparrow MA. 2006. Alkenone paleothermometry: lessons from marine sediment records off western South America. *Geochimica et Cosmochimica Acta* **70**: 101–117.

Prell WL. 1985. *The stability of low-latitude sea surface temperatures: an evaluation of the CLIMAP reconstruction with emphasis on the positive SST anomalies*, Technical Report TRO-25, US Department of Energy: Washington, DC; 1–60.

Ravelo AC. 2006. Walker circulation and global warming: lessons from the geologic past. *Oceanography* **19**: 72–80.

Rutherford S, D'Hondt S. 2000. Early onset and tropical forcing of 100,000-year Pleistocene glacial cycles. *Nature* **408**: 72–75.

Shackleton NJ, Berger A, Peltier WR. 1990. An alternative astronomical calibration of the Pleistocene timescale based on ODP Site 677. *Transactions of the Royal Society of Edinburgh: Earth Sciences* **81**: 251–261.

Spero HJ, Mielke KM, Kalve EM, *et al.* 2003. Multispecies approach to reconstructing eastern equatorial Pacific thermocline hydrography during the past 630 kyr. *Paleoceanography* **18**: 1022.

Toggweiler JR, Dixon KW, Broecker W. 1991. The Peru upwelling and the ventilation of the South Pacific thermocline. *Journal of Geophysical Research* **96**: 20467–20497.

WOA (World Ocean Atlas), version 2. 1998. Technical report, National Oceanographic Data Center: Sliver Spring, MD. http://www.nodc.-noaa.gov/oc5/woa09.html [29 August 2012].

Wyrtki K. 1966. Oceanography of the eastern equatorial Pacific Ocean. *Oceanography and Marine Biology Annual Review* **4**: 33–68.

Wyrtki K. 1977. Advection in the Peru Current as observed by satellite. *Journal of Geophysical Researches* **82**: 3939–3943.

Wyrtki K. 1981. An estimate of equatorial upwelling in the Pacific. *Journal of Physical Oceanography* **11**: 1205–1214.